Published in final edited form as:
*Tumour Biol*. 2017 May ; 39(5): 1010428317701628. doi:10.1177/1010428317701628.

# Hyaluronan-binding peptide for targeting peritoneal carcinomatosis

**Hideki Ikemoto**[1], **Prakash Lingasamy**[1], **Anne-Mari Anton Willmore**[1], **Hedi Hunt**[1], **Kaarel Kurm**[1], **Olav Tammik**[2], **Pablo Scodeller**[1], **Lorena Simón-Gracia**[1], **Venkata Ramana Kotamraju**[3], **Andrew M Lowy**[4], **Kazuki N Sugahara**[3,5], and **Tambet Teesalu**[1,3,6]

[1]Laboratory of Cancer Biology, Institute of Biomedicine and Translational Medicine, University of Tartu, Tartu, Estonia

[2]Department of Surgical Oncology, Tartu University Hospital, Tartu, Estonia

[3]Cancer Research Center, Sanford Burnham Prebys Medical Discovery Institute, La Jolla, CA, USA

[4]Department of Surgery, Division of Surgical Oncology, Moores Cancer Center, University of California, San Diego, La Jolla, CA, USA

[5]Department of Surgery, Columbia University College of Physicians and Surgeons, New York, NY, USA

[6]Center for Nanomedicine, University of California, Santa Barbara, Santa Barbara, CA, USA

## Abstract

Peritoneal carcinomatosis results from dissemination of solid tumors in the peritoneal cavity, and is a common site of metastasis in patients with carcinomas of gastrointestinal or gynecological origin. Peritoneal carcinomatosis treatment is challenging as poorly vascularized, disseminated peritoneal micro-tumors are shielded from systemic anticancer drugs and drive tumor regrowth. Here, we describe the identification and validation of a tumor homing peptide CKRDLSRRC (IP3), which upon intraperitoneal administration delivers payloads to peritoneal metastases. IP3 peptide was identified by in vivo phage display on a mouse model of peritoneal carcinomatosis of gastric origin (MKN-45P), using high-throughput sequencing of the peptide-encoding region of phage genome as a readout. The IP3 peptide contains a hyaluronan-binding motif, and fluorescein-labeled IP3 peptide bound to immobilized hyaluronan in vitro. After intraperitoneal administration in mice bearing peritoneal metastases of gastric and colon origin, IP3 peptide homed robustly to



**Corresponding author:** Tambet Teesalu, Laboratory of Cancer Biology, Institute of Biomedicine and Translational Medicine, University of Tartu, Ravila 14b, Tartu 50411, Estonia. tteesalu@sbpdiscovery.org.

**Compliance with ethical standards**

Animal experimentation procedures were approved by Estonian Ministry of Agriculture, Committee of Animal Experimentation (permit #42), and use of human tumor samples was approved by the Research Ethics Committee of the University of Tartu, Estonia (permit #243/T-27) and by the Institutional Review Board at the University of California, San Diego (#090410).

**Declaration of conflicting interests**

The author(s) declared no potential conflicts of interest with respect to the research, authorship, and/or publication of this article.


Europe PMC Funders Author Manuscripts

macrophage-rich regions in peritoneal tumors, including poorly vascularized micro-tumors. Finally, we show that IP3 functionalization conferred silver nanoparticles the ability to home to peritoneal tumors of gastric and colonic origin, suggesting that it could facilitate targeted delivery of nanoscale payloads to peritoneal tumors. Collectively, our study suggests that the IP3 peptide has potential applications for targeting drugs, nanoparticles, and imaging agents to peritoneal tumors.

### Keywords

Tumor homing peptides; intraperitoneal drug delivery; silver nanoparticles; in vivo phage display; next-generation DNA sequencing

## Introduction

Peritoneal carcinomatosis (PC) results following local dissemination and subsequent spreading of epithelial cancer cells (e.g. gastric, colon, ovarian, and pancreatic carcinoma) in the peritoneal cavity. Despite aggressive treatment that may include systemic chemotherapy, intraperitoneal (IP) chemotherapy, or multimodality treatment including cytoreductive surgery in combination with hyperthermic chemotherapy,1 the prognosis for PC patients is grim, with a median survival of only a few months.2 Compared with the systemic route, IP chemotherapy achieves high drug concentrations around peritoneal tumors with less systemic exposure3 and better access to poorly vascularized peritoneal tumor nodules.4 Issues with current IP treatments include lack of target specificity, pan-peritoneal toxicity, and fast drug clearance.5,6

We and others have used systemic in vivo peptide phage display to select for homing peptides that upon intravenous administration target tumors, inflammatory lesions, injured tissues, and normal organs.7–10 However, locoregional in vivo phage display in the peritoneal cavity is challenging due to the weak negative selection of promiscuous cellular binding peptides in non-target organs resulting in low stringency of the screens and high background. Recently, high-throughput sequencing (HTS)-assisted phage display has been used as a tool to select targeting peptides in vitro11 and in vivo.12 A key advantage of HTS for in vivo selection is that it yields comprehensive information on the representation of peptides across different target and control organs throughout the screens.

Here, we used in vivo phage display in combination with HTS of the phage genome to identify peptides that target peritoneal tumors. We identified a peptide, codenamed IP3, for delivery of molecular and nanoscale cargoes to peritoneal metastases of gastric and colon origin. IP3 contains a hyaluronic acid (HA)-binding motif and targets tumor extracellular matrix and macrophages. The peptide has potential uses for locoregional delivery of therapeutic and imaging payloads to peritoneal tumors.





Europe PMC Funders Author Manuscripts

## Results and discussion

### In vivo biopanning identifies a peritoneal tumor homing peptide, IP3

To identify peptides that target PC, we performed a combination of ex vivo/in vivo biopanning with constrained CX7C peptide library displayed on a T7 bacteriophage scaffold. PC was induced by peritoneal administration of MKN-45P cells (a human gastric cancer cell line with a high potential for peritoneal dissemination) in athymic nude mice.4 One round of ex vivo selection on excised peritoneal tumors was followed by two rounds of in vivo IP biopanning (Figure 1(a)). After in vivo selection rounds, the peptide-encoding segment of the phage genome was subjected to HTS and corresponding peptides were analyzed using custom bioinformatics tools (Phage Display Parser; canbio.ut.ee). We were interested in peptides that home to peritoneal malignant lesions and show high peritoneal tumor-to-kidney (T/K) ratio. We have chosen kidney, a retroperitoneal organ, as a control since peritoneally administered peptides likely get absorbed through the peritoneum and are excreted through the kidney. Interestingly, after three selection rounds, peptides containing cryptic CendR motif R/KXXR/K (R, arginine; K, lysine; X, any amino acid)13 and peptides with consensus CR/K$X_5$R/KC (C, cysteine) comprised 14.2% and 2.1% of the peptides in IP tumors, respectively—more than the 8.1% for R/KXXR/K and 1.7% for CR/K$X_5$R/KC found in the starting naïve library. The shift in peptide phage landscape suggested that deep-sequencing-based peptide phage display can be used for the identification of homing peptides in low-stringency/high-background screens, as in the IP screen here. Among the top 10 peptides (based on representation in IP tumor), CDAPRSRRC peptide (codenamed IP1) showed the highest T/K ratio (Figure 1(b)) and was selected for individual evaluation. In addition, the peptides containing CBX5BC motif were ranked based on their representation in the tumor and the T/K value. Among these peptides, the CKRDLSRRC peptide (IP3) was selected for individual evaluation based on its absence in the kidney in the second round and high T/K ratio in the third round (Figure 1(c)).

Annealed oligonucleotides encoding IP1 (CDAPRSRRC) and IP3 (CKRDLSRRC) peptides were back-cloned into the T7 genome for display at the C-terminus of the major coat protein, and corresponding peptide phages were purified for in vivo homing tests. Phages displaying IP1, IP3, iRGD (CRGDKGPDC, a known PC homing peptide,14,15), or a negative control insertless phage were dosed IP in MKN-45P PC mice, followed by 1 h incubation, removal of blood by perfusion, removal of unbound IP phage by extensive washing with phosphate-buffered saline (PBS), and quantitation of the bound phages in the lysate of tumors and control organs. IP3 phage showed the highest titer in MKN-45P PC lesions (Figure 2(a)). IP1 phage showed lower tumor titer than positive control phage displaying iRGD peptide and was not studied further.

### IP3 peptide interacts with HA

Peptides containing dibasic Arg–Arg motif and B$X_5$B motif (B, basic amino acid (B: lysine or arginine; X: non-acidic amino acid)) are known to bind to HA.16 HA and its cleavage products are abundant in solid tumors and contribute to malignant progression and drug resistance.17,18 In fact, HA is prominently expressed in peritoneal MKN-45P tumors, especially in the tumor periphery (Figure 2(b)). HA is abundantly expressed in other

peritoneal tumors of mouse and human (Figure S1). We evaluated the interaction of IP3 peptide with HA in a cell-free system and found that 5(6)-carboxyfluorescein (FAM)-labeled IP3 peptide bound to immobilized HA ~6.4-fold over control heptaglycine peptide (Figure 2(c)). The interaction of the IP3 peptide with HA was specific: Binding of FAM-labeled IP3 peptide with HA was blocked by hyaluronidase (HAase) pretreatment but not by pretreatment with heat-inactivated HAase (Figure S2). Furthermore, the IP3/HA interaction was not affected by including up to 100 μM heparan sulfate in the binding mix (not shown). HA interacts with aggrecan/chondroitin sulfate proteoglycan-1 and link protein through ionic interactions with basic amino acids, arginine, and lysine.19 IP3 peptide CKRDLSRRC contains an LSRR motif that is similar to the LSRPR motif found in the link protein.20 The synthetic RYPLSRPRKR peptide derived from the link protein inhibits the binding of link protein to HA.20 Importantly, polylysine is not able to inhibit the interaction, suggesting that positive charge alone is not enough for the interaction with HA.20

### IP3 peptide homes to peritoneal tumors

IP inoculation of nude mice with MKN-45P cells results in growth of tumor nodules of different sizes over the peritoneal surfaces. Typically, we observed 1–2 large tumors with a diameter of ~1 cm accompanied by smaller nodules at the omentum, and multiple small nodules on the mesentery. Biodistribution of FAM-labeled synthetic IP3 peptide (FAM-IP3) in the MKN-45P PC mice was assessed after IP injection of the peptide. Four hours after injection, the unbound peptide was washed away with PBS after necropsy and fluorescence in tumors and control organs was evaluated macroscopically and microscopically. A robust macroscopic FAM signal was observed in discrete areas in both larger tumors and small nodules, while minimal background signals were seen in non-tumor tissues (Figure 3(a) and (b)). Only a minor signal was observed in tumors when a control FAM-G7 peptide was injected (Figure S3). Confocal imaging revealed that FAM-IP3 peptide accumulated in tumor areas distant from CD31-positive blood vessels (arrows in Figure 3(c) and (d)). Confocal imaging also revealed a weak FAM-IP3 signal in subcutaneous (sc) tumors (Figure S4 left). HA is an exclusively extracellular molecule and contain a large number of binging sites for link protein. One possible mechanism for remarkable ability of IP3 peptide to penetrate IP tumor lesions could be that IP3 peptide binds to and remains associated with HA it encounters at the tumor periphery, allowing free IP3 peptide to move further to reach HA deeper the tumor tissue. Detailed understanding of the deep penetration will require dedicated follow-up studies.

Immunostaining of peritoneal tumors from mice injected with FAM-IP3 peptide with anti-CD11b antibody, a marker for macrophages, showed an extensive regional overlap with the FAM-IP3 signal (Figure 4(a)–(c)). In contrast, control FAM-G7 peptide showed only background accumulation in the tumor periphery and no overlap with the CD11b staining (Figure 4(d)–(f)). Tumor-associated macrophages play important roles in tumor progression.21 Recently, Yamaguchi et al.22 reported that M2 macrophages accelerate growth of MKN-45 cells in in vitro co-culture systems and in mice. HA is recruited to macrophages and internalized through receptors such as CD4423 and HA receptors for endocytosis (HARE/Stab2).24

### IP3-silver nanoparticles home to peritoneal gastric and colon tumors

To study the potential of IP3 peptide as a targeting ligand for nanoparticles (NPs), biotinylated IP3 peptides were coupled to ~30 nm silver nanoparticles (AgNPs25). Peptide-functionalized AgNPs were injected IP into mice bearing PC created with gastric (MKN-45P) and colon (CT26) cancer cells. Confocal images revealed a robust accumulation of IP3-AgNPs in the outer rim of both MKN-45P and CT26 tumors (Figure 5(a) and (b)). In addition to the peripheral accumulation, IP3-AgNPs penetrated deeper into the tumor (arrows in Figure 5(a)). In contrast to IP3-AgNPs, only low, background levels of the control AgNPs (biotin without peptide) were observed at the edge of both MKN-45P and CT26 tumors (arrowheads in Figure 5(c) and (d)).

To evaluate translational potential of IP3-AgNPs, we tested the binding of the NPs to surgical explants of peritoneal tumors of colon cancer in ex vivo tumor dipping assays.26,27 IP3-AgNPs bound to the periphery of the tumors (Figure 6(a)), whereas the control AgNPs did not (Figure 6(b)). Restriction of IP3 NPs to the outer rim of tumors could be due to bulkiness of the particles and due to “avidity barrier”—particles displaying multiple peptides being immobilized due to multiple low-affinity interactions. The effect of NP size and density of IP3 peptide on the penetration remains a subject of follow-up studies.

In conclusion, this study resulted in the identification of the IP3 peptide, a novel ligand for peritoneal tumor targeting. Our data show that IP3 delivers a low molecular weight compound (FAM) deep into peritoneal tumors, whereas it only allows NPs (AgNPs) to penetrate the tumor periphery. This difference in penetration depth could be attributed to cargo size (FAM vs AgNPs). However, binding-site barrier effect—high affinity/avidity targeting ligands being trapped near tumor entry sites28—may also contribute to the poor tumor penetration of IP3-AgNPs given the multivalent interaction between ~100 copies of IP3 peptides on the NP surface and HA at the tumor periphery. In fact, CD44, a natural HA ligand, binds irreversibly to high molecular weight HA when multivalent interaction takes place.29 Nonetheless, the IP3 peptide may be a powerful tool for peritoneal tumor-specific targeting through the abdominal cavity, and provide an opportunity to improve the detection and treatment of PC.

## Materials and methods

### Materials

$CHCl_3$, MeOH, isopropanol, and dimethylformamide (DMF) were purchased from Sigma-Aldrich. PBS was purchased from Lonza (Belgium). Peptides were synthesized using Fmoc/t-Bu chemistry on a microwave-assisted automated peptide synthesizer (Liberty; CEM Corporation, Matthews, NC, USA). Peptides were purified by high-performance liquid chromatography (HPLC) using 0.1% trifluoroacetic acid (TFA) in acetonitrile–water mixtures to 90%–95% purity and validated by quadrupole time-of-flight (Q-TOF) mass spectral analysis. Fluorescent peptides were synthesized by using FAM with 6-aminohexanoic acid spacer. FAM-G7 was purchased from TAG Copenhagen (Frederiksberg, Denmark).

### Cell lines and mouse models

MKN-45P human gastric cancer cells were isolated from parental MKN-45.30 CT26 cell lines were purchased from American Type Culture Collection (CT.26 ATCC CLR-2638; ATCC, United Kingdom). Cell lines were used without further authentication. The cells were cultivated in Dulbecco's Modified Eagle's Medium (DMEM; Lonza) with 100 IU/mL of penicillin, streptomycin, and 10% of heat-inactivated fetal bovine serum (FBS; GE Healthcare, United Kingdom). Nude mice were intraperitoneally injected with $2 \times 10^6$ MKN-45P cells and Balb/c mice with $2 \times 10^6$ CT26 cells. For dual tumors, nude mice were simultaneously injected intraperitoneally with $2 \times 10^6$ MKN-45P cells and subcutaneously with $2 \times 10^5$ MKN-45P cells in the right flank. The MKN-45P tumors were grown for 2 weeks and the CT26 tumors for 1 week. Athymic nude mice and Balb/c mice were purchased from Harlan Sprague Dawley (HSD, Indianapolis, IN, USA).

### T7 phage peptide library biopanning

A combination of ex vivo and in vivo T7 peptide phage biopanning was used to identify peptides that target PC lesions.10 Briefly, T7Select Phage Display System (EMD Biosciences, Gibbstown, NJ, USA) with T7 vector 415-1b was used to construct cyclic CX7C phage libraries (diversity ~$10^8$) and for individual phage cloning according to the manufacturer's instructions. Phage was amplified in *Escherichia coli* (BLT5403; EMD Biosciences) and purified by precipitation with PEG-8000 (Sigma-Aldrich, St. Louis, MO, USA), followed by $CsCl_2$ gradient ultracentrifugation and dialysis.10 For ex vivo biopanning, $10^{10}$ pfu of CX7C phage naïve library was incubated with tumor and organs excised from the mice with MKN-45 IP tumors. After the incubation for 1 h, the tissues were washed with DMEM and transferred in lysogeny broth (LB) bacterial growth medium containing 1% NP40 (LB-NP40). For in vivo biopanning, amplified phage pool from previous round was IP injected to an MKN-45 tumor mouse and incubated for 1 h. After the termination, tumors and organs were collected, washed with DMEM, and transferred in LB-NP40. The rescued phage was amplified, pooled, and used for the subsequent round of selection. Phage was quantified using plaque assay, and the sequences of phage-displayed peptides were inferred from the DNA encoding the insert-containing region at the C-terminus of the T7 major coat protein gp10.

### Peptide binding assay

The binding of peptides to immobilized HA was studied by an enzyme-linked immunosorbent assay (ELISA)-type phage binding assay. Ninety-six-well plates (Corning Life Sciences, Tewksbury, MA, USA) were coated with 100 μL of 200 μg/mL HA (cat. no. 53747; Sigma-Aldrich) in PBS at 4°C overnight, washed three times with PBS, blocked with 300 μL of blocking solution (1× PBS, 1% bovine serum albumin (BSA), 0.1% Tween®-20) for 1 h at 37°C, and washed three times with blocking solution. For HAase treatment, HAase in PBS (stock 1 mg/mL) was combined with 20 μg of dissolved HA in PBS and incubated at 37°C for 2 h. For heat inactivation, HAase was incubated at 100°C for 10 min. For IP3 binding, 100 μL of peptide solution in blocking solution was added to each well (10 μg peptide/well), incubated at room temperature for 4–6 h, and washed three times with blocking solution. Primary antibody, rabbit anti-FAM (cat. no. A889; diluted in 1: 5000),

was added to each well and incubated at 37°C for 1 h and washed three times with blocking solution. Next, anti-rabbit-HRP (horseradish peroxidase) conjugate (1:10,000; Jackson ImmunoResearch) was added at 100 μL per well, incubated at 37°C for 1 h, and washed four times with blocking solution. The peroxidase reaction was done by adding 100 μL/well of freshly prepared solution from TMB Peroxidase EIA Substrate Kit (Bio-Rad, Hercules, CA, USA), followed by incubation at 37°C for 5 min. The reaction was stopped by 1 N $H_2SO_4$, and absorbance was measured at 450 nm with a microplate reader (Tecan Austria GmbH, Salzburg, Austria).

### HTS of phage genomic DNA

Tissue lysates were amplified and DNA was extracted using a DNA extraction kit (High Pure PCR Template Preparation Kit; Roche, Basel, Switzerland). The extracted DNA was subjected to HTS using the Ion Torrent next-generation sequencing system (Thermo Fisher Scientific, Waltham, MA, USA).

### AgNP synthesis and functionalization

AgNPs with CF555 dye–labeled neutravidin coating (555-Ag-NA) were prepared as described in Pang et al.25 with the difference that AgNPs were synthesized by citrate reduction with a core size of ~30 nm Ag rather than polyvinylpyrrolidone reduction. An extinction of $8.8 \times 10^9$ $M^{-1}$ $cm^{-1}$ at the 405-nm Ag plasmon peak was used to quantify the concentration of AgNPs. Particles were functionalized with biotinylated peptides as described earlier.31

### In vivo biodistribution studies

FAM-labeled peptides of 100 nmol in 0.5 mL PBS was intraperitoneally injected into tumor-bearing mice. After 4 h, the mice were sacrificed under deep anesthesia. Tissues were harvested, rinsed with PBS to remove unbound peptide, imaged under an Illuminatool Bright Light System LT-9900 (Lightools Research, Encinitas, CA, USA), and processed for immunostaining. For NPs, AgNPs or IP3-AgNPs (40 optical density (O.D.)) in PBS were intraperitoneally injected into tumor-bearing mice. After 4 h, the mice were sacrificed under deep anesthesia. Tissues were harvested, rinsed with PBS to remove unbound NPs, and snap-frozen in liquid nitrogen.

### Immunofluorescence and microscopic imaging

The excised tumor and organs were snap-frozen in liquid nitrogen, cryosectioned at 10 μm, fixed with 4% paraformaldehyde for 10 min at room temperature (RT), and immunostained with anti-fluorescein rabbit immunoglobulin G (IgG) fragment (Thermo Fisher Scientific, Waltham, MA, USA), rat anti-mouse CD31 and CD11b (BD Biosciences, Franklin Lakes, NJ, USA) as primary antibodies, and Alexa Fluor 488 goat anti-rabbit IgG and Alexa Fluor 647 goat anti-rat IgG (Thermo Fisher Scientific, Waltham, MA, USA) as secondary antibodies. The nuclei of cells were stained with 4′,6-diamidino-2-phenylindole (DAPI; 5 μL/mL, 10 min). Images of the tissue sections were taken with confocal microscopy (Olympus FV1200MPE, Hamburg, Germany).

### Ex vivo tumor dipping assay

Fresh surgical samples of peritoneal metastases of colon cancer were collected and immediately divided in explants of around 1 $cm^3$ and incubated in DMEM containing 1% of BSA and AgNPs or IP3-AgNPs at 37°C for 4 h. After three washes with PBS, the tumors were snap-frozen in liquid nitrogen.

## Supplementary Material

Refer to Web version on PubMed Central for supplementary material.

## Acknowledgements

The authors thank Dr Erkki Ruoslahti for the advice, Dr Joji Kitayama for kind gift of MKN-45P cells, and Rein Laiverik for help with characterization of the silver nanoparticles (AgNPs).

**Funding**

The author(s) disclosed receipt of the following financial support for the research, authorship, and/or publication of this article: This work was supported by the European Union through the European Regional Development Fund (Project No. 2014-2020.4.01.15-0012), by EMBO Installation grant #2344 (to T.T.), European Research Council starting grant GLIOMADDS from European Regional Development Fund (to T.T.), Wellcome Trust International Fellowship WT095077MA (to T.T.), and National Cancer Institute (NCI) of National Institutes of Health (NIH) grant R01CA167174 (to K.N.S.).

## References

1. Lengyel E. Ovarian cancer development and metastasis. Am J Pathol. 2010; 177(3):1053–1064. [PubMed: 20651229]
2. Montori G, Coccolini F, Ceresoli M, et al. The treatment of peritoneal carcinomatosis in advanced gastric cancer: state of the art. Int J Surg Oncol. 2014; 2014:912418. [PubMed: 24693422]
3. Bajaj G, Yeo Y. Drug delivery systems for intraperitoneal therapy. Pharm Res. 2010; 27:735–738. [PubMed: 20198409]
4. Emoto S, Yamaguchi H, Kishikawa J. Antitumor effect and pharmacokinetics of intraperitoneal NK105, a nanomicellar paclitaxel formulation for peritoneal dissemination. Cancer Sci. 2012; 103:1304–1310. [PubMed: 22429777]
5. Lu Z, Wang J, Wientjes MG, et al. Intraperitoneal therapy for peritoneal cancer. Future Oncol. 2010; 6:1625–1641. [PubMed: 21062160]
6. Ceelen, WP., Levine, E. Intraperitoneal cancer therapy: principles and practice. Boca Raton, FL: CRC Press; 2015.
7. Ruoslahti E. Specialization of tumour vasculature. Nat Rev Cancer. 2002; 2(2):83–90. [PubMed: 12635171]
8. Kelly KA, Nahrendorf M, Amy MY, et al. In vivo phage display selection yields atherosclerotic plaque targeted peptides for imaging. Mol Imaging Biol. 2006; 8(4):201–207. [PubMed: 16791746]
9. Mann AP, Scodeller P, Hussain S, et al. A peptide for targeted, systemic delivery of imaging and therapeutic compounds into acute brain injuries. Nat Commun. 2016; 7:11980. [PubMed: 27351915]
10. Teesalu T, Sugahara KN, Ruoslahti E. Mapping of vascular ZIP codes by phage display. Methods Enzymol. 2012; 503:35–56. [PubMed: 22230564]
11. Liu GW, Livesay BR, Kacherovsky NA. Efficient identification of murine M2 macrophage peptide targeting ligands by phage display and next-generation sequencing. Bioconjug Chem. 2015; 26(8): 1811–1817. [PubMed: 26161996]
12. Urich E, Schmucki R, Ruderisch N, et al. Cargo delivery into the brain by in vivo identified transport peptides. Sci Rep. 2015; 5:14104. [PubMed: 26411801]

13. Teesalu T, Sugahara KN, Kotamraju VR, et al. C-end rule peptides mediate neuropilin-1-dependent cell, vascular, and tissue penetration. Proc Natl Acad Sci U S A. 2009; 106(38):16157–16162. [PubMed: 19805273]
14. Sugahara KN, Scodeller P, Braun GB, et al. A tumor-penetrating peptide enhances circulation-independent targeting of peritoneal carcinomatosis. J Control Release. 2015; 212:59–69. [PubMed: 26071630]
15. Simon-Gracia L, Hunt H, Scodeller P, et al. iRGD peptide conjugation potentiates intraperitoneal tumor delivery of paclitaxel with polymersomes. Biomaterials. 2016; 104:247–257. [PubMed: 27472162]
16. Amemiya K, Nakatani T, Saito A, et al. Hyaluronan-binding motif identified by panning a random peptide display library. Biochim Biophys Acta. 2005; 1724(1–2):94–99. [PubMed: 15921857]
17. Stern R, Asari AA, Sugahara KN. Hyaluronan fragments: an information-rich system. Eur J Cell Biol. 2006; 85(8):699–715. [PubMed: 16822580]
18. Dicker KT, Gurski LA, Pradhan S. Hyaluronan: a simple polysaccharide with diverse biological functions. Acta Biomater. 2014; 10(4):1558–1570. [PubMed: 24361428]
19. Roberts JJ, Elder RM, Neumann AJ. Interaction of hyaluronan binding peptides with glycosaminoglycans in poly(ethylene glycol) hydrogels. Biomacromolecules. 2014; 15(4):1132–1141. [PubMed: 24597474]
20. Goetinck PF, Stirpe NS, Tsonis PA. The tandemly repeated sequences of cartilage link protein contain the sites for interaction with hyaluronic acid. J Cell Biol. 1987; 105(5):2403–2408. [PubMed: 2445761]
21. Noy R, Pollard JW. Tumor-associated macrophages: from mechanisms to therapy. Immunity. 2014; 41(1):49–61. [PubMed: 25035953]
22. Yamaguchi T, Fushida S, Yamamoto Y, et al. Tumor-associated macrophages of the M2 phenotype contribute to progression in gastric cancer with peritoneal dissemination. Gastric Cancer. 2016; 19(4):1052–1065. [PubMed: 26621525]
23. Tran TH, Rastogi R, Shelke J, et al. Modulation of macrophage functional polarity towards anti-inflammatory phenotype with plasmid DNA delivery in CD44 targeting hyaluronic acid nanoparticles. Sci Rep. 2015; 5:16632. [PubMed: 26577684]
24. Micale N, Piperno A, Mahfoudh N, et al. A hyaluronic acid–pentamidine bioconjugate as a macrophage mediated drug targeting delivery system for the treatment of leishmaniasis. RSC Adv. 2015; 5:95545–95550.
25. Pang HB, Braun GB, Friman T, et al. An endocytosis pathway initiated through neuropilin-1 and regulated by nutrient availability. Nat Commun. 2014; 5:4904. [PubMed: 25277522]
26. Sugahara KN, Teesalu T, Karmali PP, et al. Coadministration of a tumor-penetrating peptide enhances the efficacy of cancer drugs. Science. 2010; 328(5981):1031–1035. [PubMed: 20378772]
27. Braun GB, Sugahara KN, Yu OM, et al. Urokinase-controlled tumor penetrating peptide. J Control Release. 2016; 232:188–195. [PubMed: 27106816]
28. Fujimori K, Covell DG, Fletcher JE. A modeling analysis of monoclonal antibody percolation through tumors: a binding-site barrier. J Nucl Med. 1990; 31:1191–1198. [PubMed: 2362198]
29. Wolny PM, Banerji S, Gounou C, et al. Analysis of CD44-hyaluronan interactions in an artificial membrane system insights into the distinct binding properties of high and low molecular weight hyaluronan. J Biol Chem. 2010; 285(39):30170–30180. [PubMed: 20663884]
30. Koga A, Aoyagi K, Imaizumi T, et al. Comparison between the gastric cancer cell line MKN-45 and the high-potential peritoneal dissemination gastric cancer cell line MKN-45P. Kurume Med J. 2011; 58(3):73–79. [PubMed: 22531121]
31. Paasonen L, Sharma S, Braun GB. New p32/gC1qR ligands for targeted tumor drug delivery. ChemBioChem. 2016; 17(7):570–575. [PubMed: 26895508]

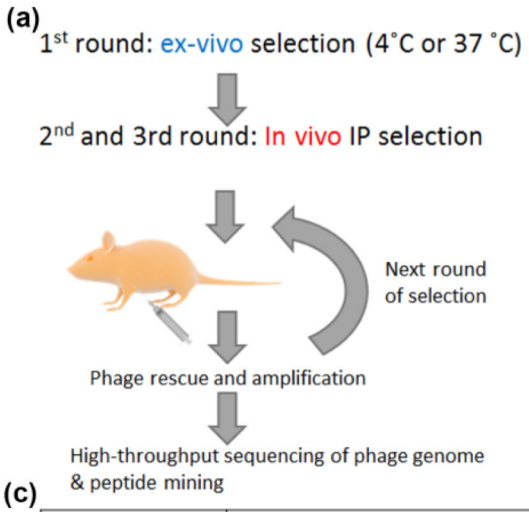


(b)

| | | R3 | | | |
|---|---|---|---|---|---|
| | | i.p. tumor | Kidney | s.c. tumor | |
| Unique peptides | | 36250 | 25867 | 15880 | |
| Total peptides | | 150439 | 128119 | 221299 | |
| Rank | Peptide sequence | | | | T/K |
| 1 | CKKKAGSGC | 57 | 83 | 15 | 0.64 |
| 2 | CKELRDMQC | 54 | 80 | 45 | 0.63 |
| IP1-> 3 | CDAPRSRRC | 47 | 2 | 0 | 21.89 |
| 4 | CKGKGRKGC | 41 | 56 | 38 | 0.68 |
| 5 | CGKKESPRC | 40 | 18 | 2 | 2.07 |
| 6 | CNKSMRNSC | 39 | 23 | 2 | 1.58 |
| 7 | CNKQARAKC | 38 | 69 | 15 | 0.51 |
| 8 | CERAQNGGC | 37 | 24 | 84 | 1.44 |
| 9 | CTGRDGKSC | 36 | 55 | 123 | 0.61 |
| 10 | CVNQVGKRC | 35 | 50 | 209 | 0.65 |

(c)

| | R3 | | | |
|---|---|---|---|---|
| Peptide sequence | i.p. tumor | Kidney | s.c. tumor | T/K |
| CRKVKGDKC | 30 | 36 | 2 | 0.71 |
| CKKGLKGKC | 20 | 18 | 225 | 0.95 |
| CREGKGVRC | 20 | 20 | 28 | 0.85 |
| CKKKESSRC | 18 | 2 | 0 | 7.66 |
| CKGGKGARC | 16 | 62 | 18 | 0.22 |
| CRDTGEEKC | 16 | 21 | 159 | 0.65 |
| CKSEHVKKC | 16 | 14 | 20 | 0.97 |
| CKGKNSGRC | 15 | 9 | 32 | 1.42 |
| CKKSGGKKC | 15 | 77 | 0 | 0.17 |
| CKGAEEKKC | 15 | 2 | 16 | 6.39 |
| CREKRDNKC | 14 | 4 | 0 | 2.98 |
| CRSNMREKC | 13 | 3 | 3 | 3.69 |
| CKRDLSRRC | 13 | 2 | 0 | 5.54 |
| CRGSVNKRC | 13 | 5 | 0 | 2.21 |

| | R2 Kidney | |
|---|---|---|
| | M1 | M2 |
| CKKKESSRC | 13 | 10 |
| CKRDLSRRC | 0 | 0 |

<-IP3

**Figure 1.**

Screening for peritoneal tumor homing peptides by in vivo phage display. (a) Flow of biopanning screens. Naïve CX7C library was first selected ex vivo by incubation with tumor explants for 1 h at 37°C or at 4°C, followed by two rounds of in vivo selection. (b) Recovered peptides were ranked based on the count of high-throughput sequencing reads and on T/K ratio. Among the top 10 peptides, a peptide with a highest T/K ratio, CDAPRSRRC (designated IP1), was selected for further evaluation. (c) Peptides with consensus CBX5BC (C, cysteine; B, basic amino acid) were ranked based on the number of their representation in IP tumors. CKRDLSRRC (designated IP3) was selected based on its low representation in the kidney in the second round.




Europe PMC Funders Author Manuscripts

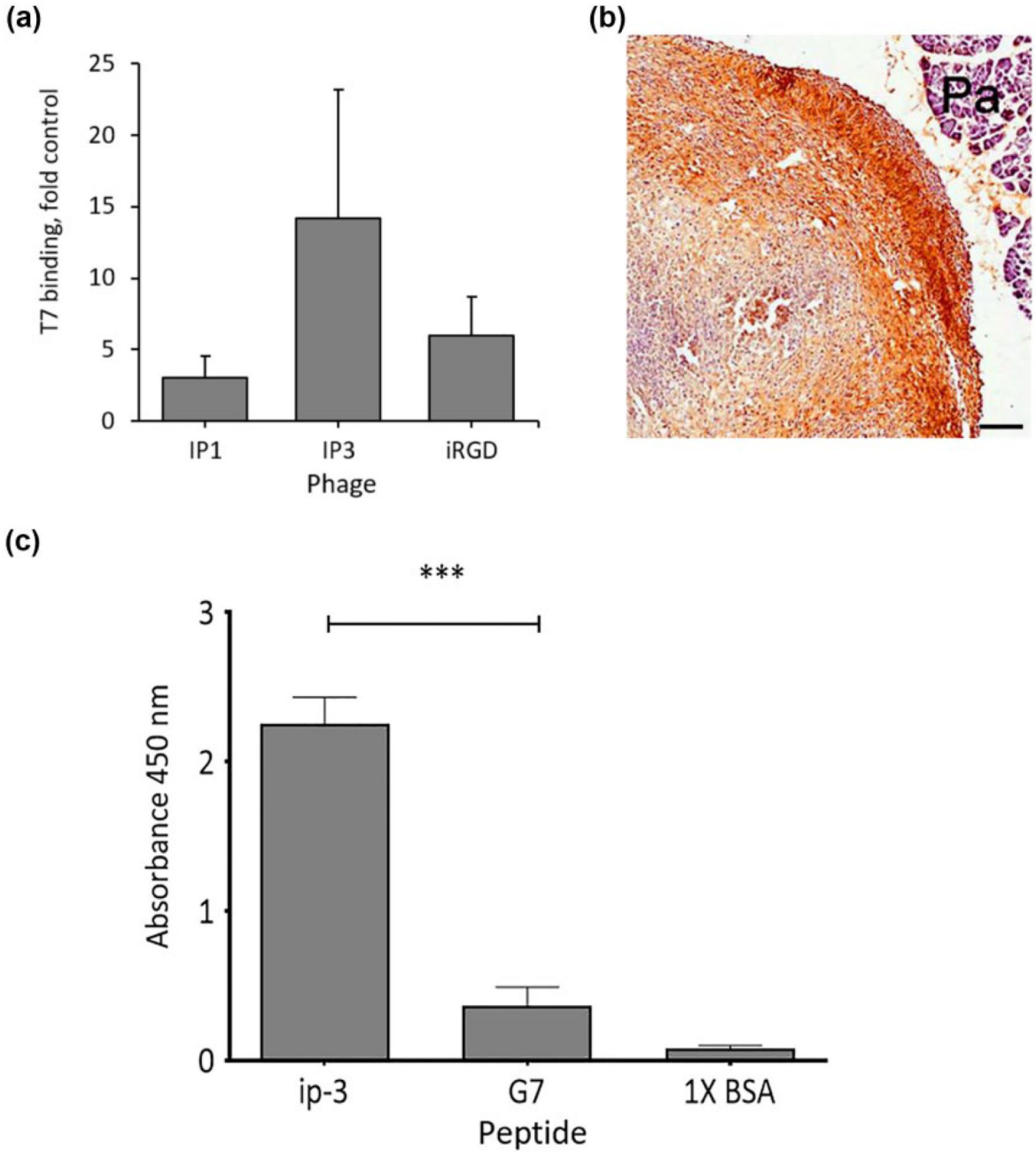


**Figure 2.**

IP3 peptide homes to MKN-45P tumors and interacts with HA in a cell-free system. (a) IP1, IP3, and iRGD (positive control peptide) phages were evaluated by in vivo dosing of MKN-45P tumor mice. Titers of peritoneal tumor samples are expressed fold over insertless negative control phage. Error bars: SEM, n = 3. (b) HA is abundantly expressed in the periphery of MKN-45P tumors. The tumors were sectioned and incubated with biotinylated antibody against hyaluronan-binding protein followed by incubation with streptavidin linked to peroxidase and colorimetric diaminobezidine reaction. Pa, pancreas. Scale bar: 200 μm.




Europe PMC Funders Author Manuscripts

(c) IP3 peptide binds to immobilized HA. FAM-IP3 peptide was incubated with ELISA plates coated with HA, followed by incubations with anti-FAM antibody as primary antibody and rabbit-HRP conjugate as secondary antibody, and a chromogenic color reaction. Statistical analysis was performed by Student unpaired t-test. Error bars: SEM, n= 8, ***$p < 0.001$.



Europe PMC Funders Author Manuscripts

Europe PMC Funders Author Manuscripts

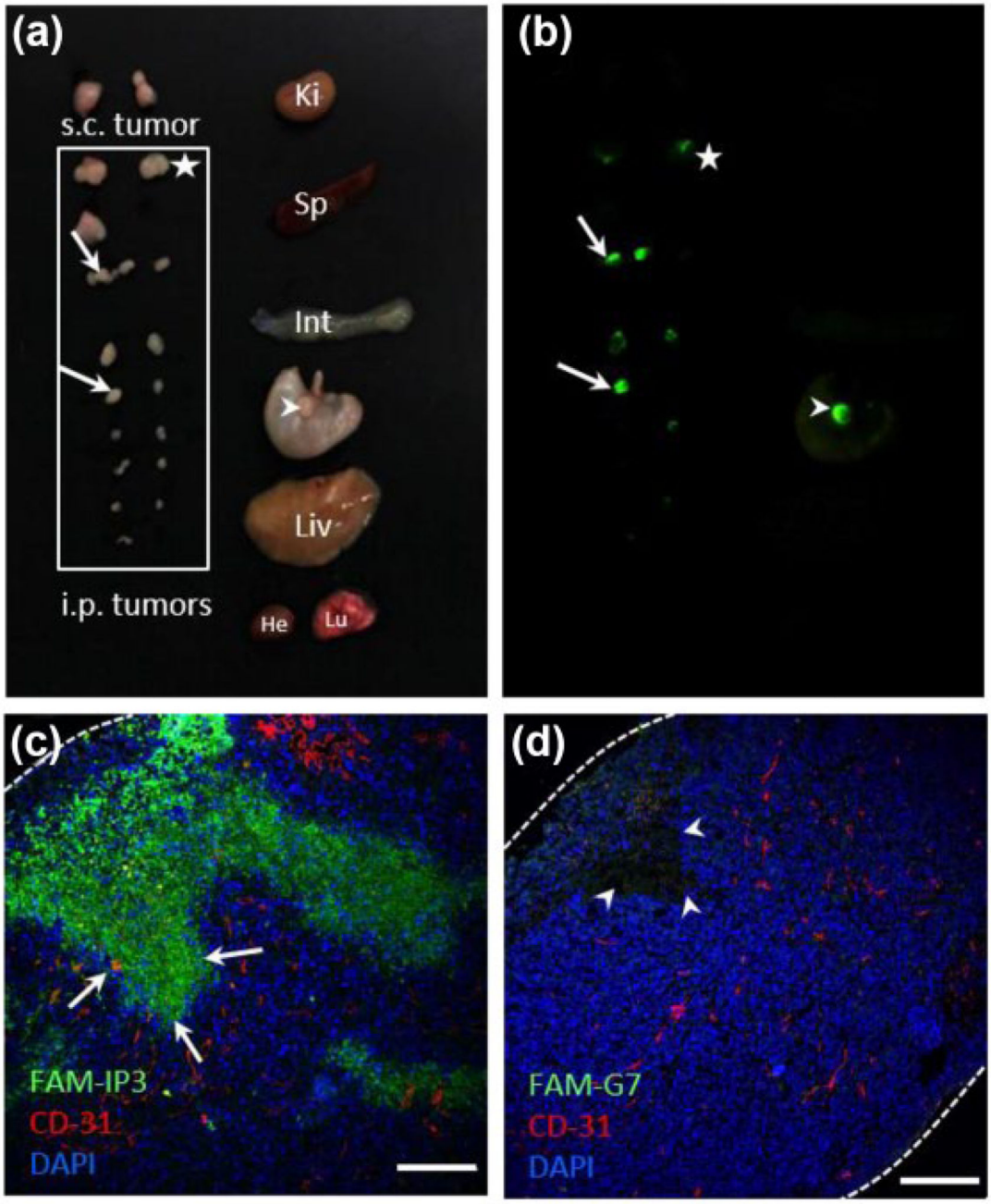


**Figure 3.**

Synthetic intraperitoneally administered IP3 peptide homes to MKN-45P tumors. MKN-45P tumor mice were injected intraperitoneally with 100 nmol of FAM-labeled IP3 (FAM-IP3) peptide. After 4 h, the mice were intravenously perfused with PBS and the peritoneal space was flushed with PBS. Tissues were collected for macroscopic imaging with Illumatool (Lightools Research, Encinitas, CA, USA), followed by snap-freezing, sectioning, immunostaining, and confocal imaging. (a) A white-light view of excised tumors and control organs and (b) corresponding FAM image. Representative images selected from three

independent experiments are shown. Strong fluorescence was observed in discrete areas of larger tumors (e.g. tumor with star) and in small nodules (arrows). Arrowhead points to a small tumor nodule attached to the stomach. Organs: Ki, kidney; Sp, spleen; Int, intestine; St, stomach; Liv, liver; He, heart; Lu, lung. (c) and (d): Green: FAM-IP3 or FAM-G7; red: CD31 (blood vessels); blue: DAPI. Scale bar: 200 μm. (c) Confocal imaging demonstrated the presence of tumor FAM-IP3 signal in discrete areas (arrows). (d) A confocal image of a tumor from an MKN-45P tumor mouse dosed with 100 nmol FAM-G7 peptide shows no detectable FAM-G7 peptide.



Europe PMC Funders Author Manuscripts

Europe PMC Funders Author Manuscripts

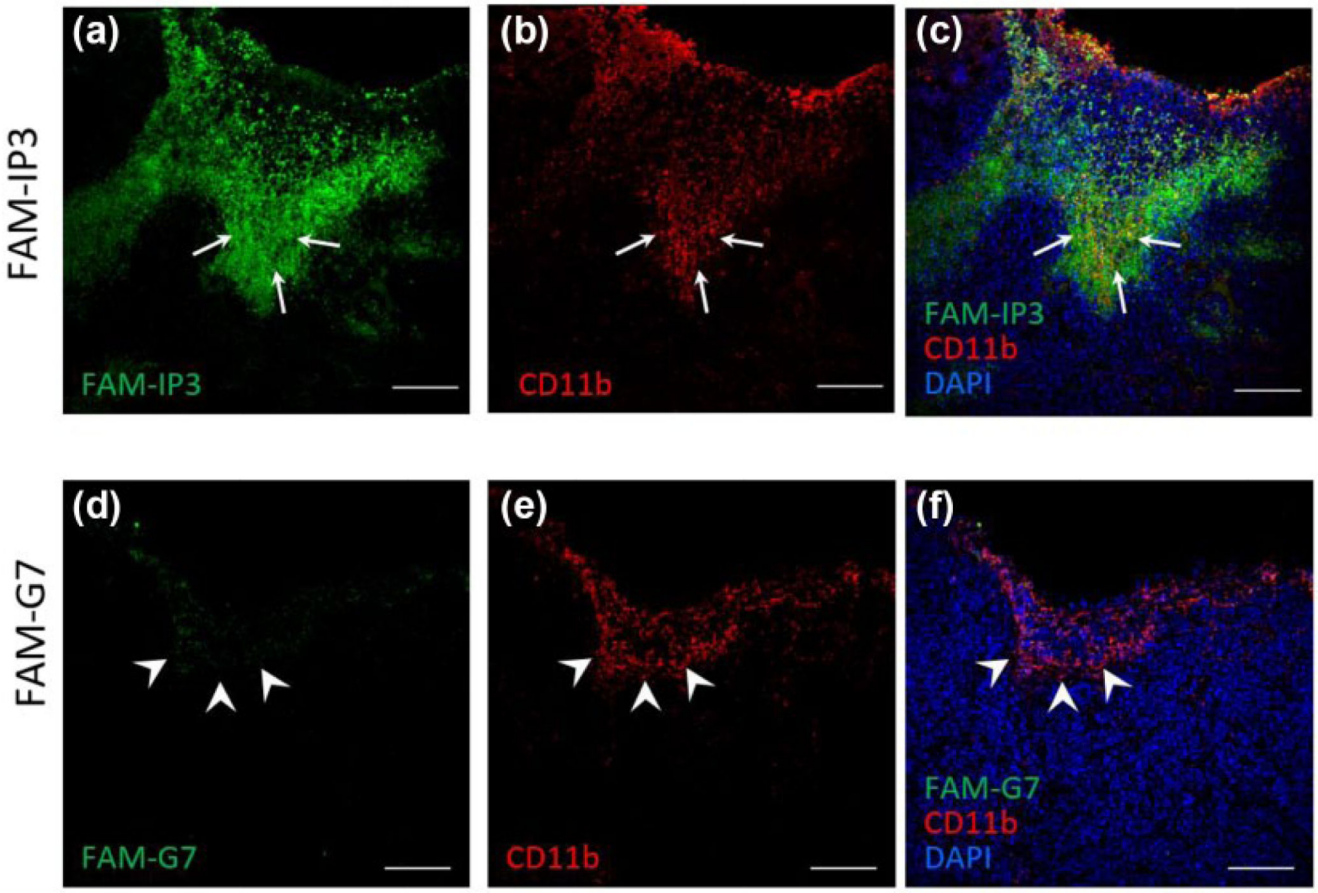


**Figure 4.**

IP-administered IP3 peptide homes to tumor areas rich in macrophages. The sections of MKN-45P tumor IP injected with 100 nmol of FAM-IP3 peptide (upper row) or FAM-G7 peptide (lower row) were immunostained with anti-CD11b. (a)–(c) FAM-IP3 signal (green, upper row) overlaps with the CD11b signal (red). (d)–(f) FAM-G7 peptide showed no overlap with the CD11b staining. The arrowheads point to an area rich in macrophages. Green: FAM-IP3 or FAM-G7; red: CD11b; blue: DAPI. Scale bar: 200 μm.

Europe PMC Funders Author Manuscripts

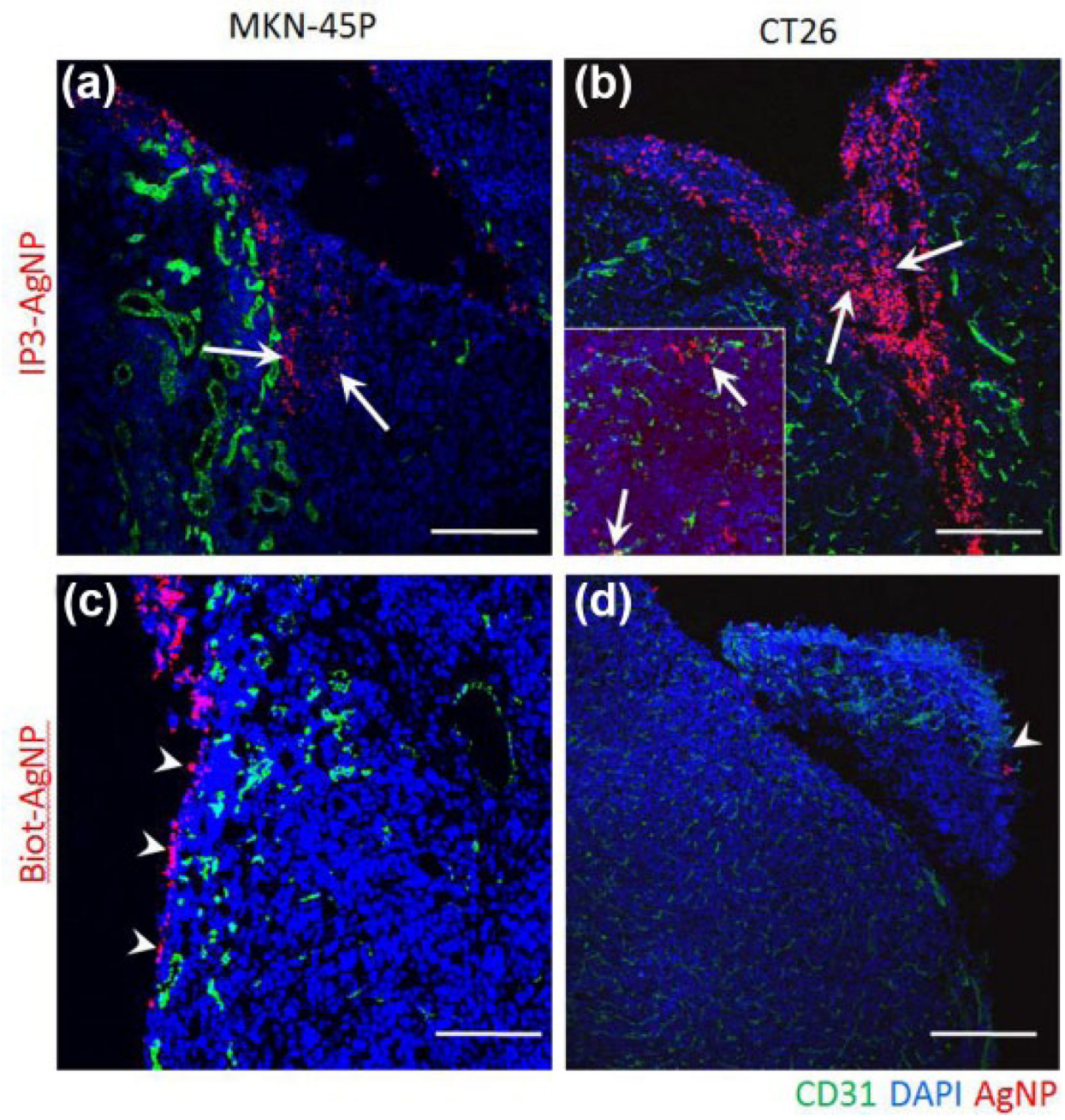


**Figure 5.**

IP-administered IP3 peptide-conjugated AgNPs home to peritoneal gastric and colon carcinomas. Confocal imaging of MKN-45P and CT26 tumors after 4 h of injection with AgNPs (red). The cryosections were immunostained with anti-CD31 (green) and the nuclei were counterstained with DAPI (blue). (a) and (b) Tumor homing and penetration of IP3-AgNPs. (a) IP3-AgNPs located away from the edge of the tumor to some degree while being associated with blood vessel or without association with blood vessel (arrows). (b) IP3-AgNPs were found associated with blood vessels and accumulated in the avascular regions.

Arrows point to IP3-AgNPs in an avascular region. Inset in (b): IP3-AgNPs overlapped with blood vessels inside the tumor (arrows). (c) and (d) Imaging of control nanoparticles. The control AgNPs located on the edge of the tumor for both (c) MKN-45P and (d) CT26 tumors (arrows). (a)–(d): Red, AgNPs; green, CD31; blue, DAPI. Scale bar in (a), (c), and (d): 200 μm; and in (b): 100 μm.



Europe PMC Funders Author Manuscripts

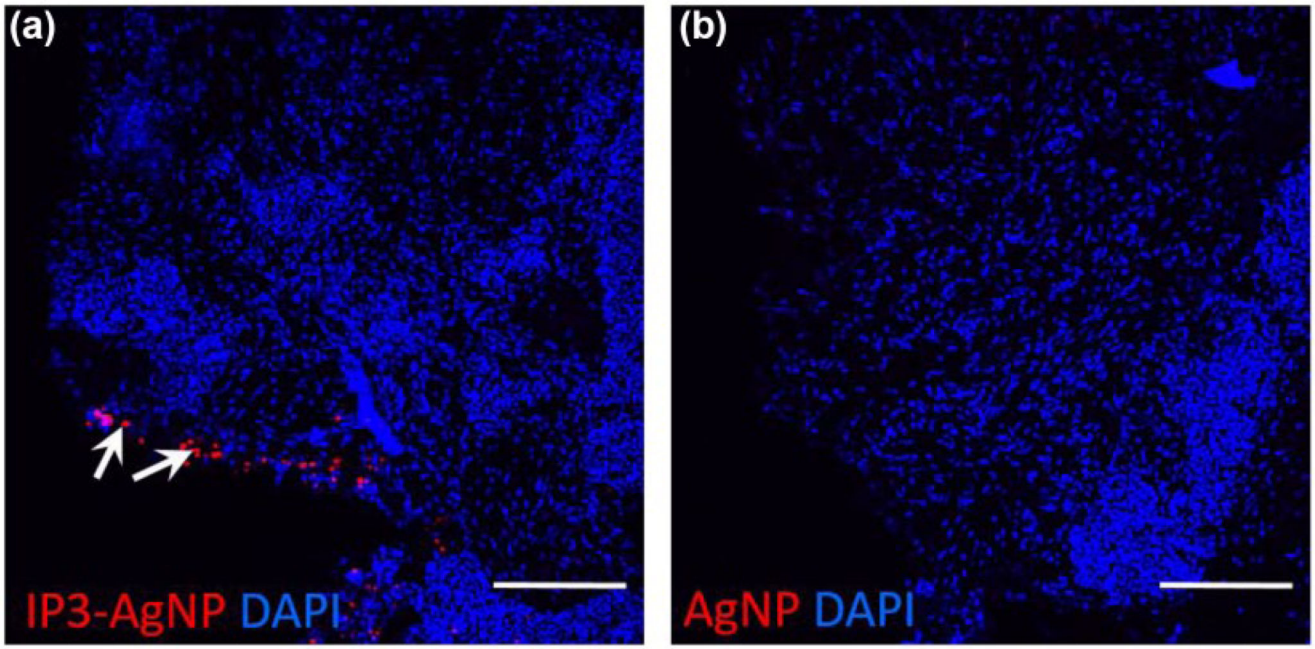


**Figure 6.**

IP3-AgNPs accumulate in a surgically excised peritoneal tumor explant. IP3-AgNPs accumulated in the periphery of the human colon carcinoma explants. Arrows point to IP3-AgNPs bound on the edge of the tumor. (a) and (b): Red, IP3-AgNPs or AgNPs; blue, DAPI. Scale bars: 200 μm.



Europe PMC Funders Author Manuscripts